Surface-Enhanced Infrared Spectroscopy: A Comparison of Metal Island Films with Discrete and Nondiscrete Surface Plasmons

T. R. JENSEN, R. P. VAN DUYNE,* S. A. JOHNSON, and V. A. MARONI*

Department of Chemistry, Northwestern University, Evanston, Illinois 60208 (T.R.J., R.P.V.D.); and Argonne National Laboratory, Argonne, Illinois 60439 (S.A.J., V.A.M.)

A study of the surface-enhanced infrared absorption (SEIRA) spectroscopy of *para*-nitrobenzoic acid (PNBA) adsorbed on thermally evaporated silver films has been conducted to determine the effect of film architecture on the magnitude of the SEIRA enhancement. Ordered arrays of uniformly sized silver nanoparticles, termed periodic particle arrays (PPAs), were prepared on several different infrared transparent substrates (germanium, silicon, and mica) by nanosphere lithography (NSL). It was found that the ordered arrays deposited by NSL produced well-defined and intense surface plasmon resonance (SPR) bands in the infrared at frequencies between 1500 and 4000 cm^{-1}. The peak frequency of these infrared SPR bands depended on the array architecture and the substrate material. By appropriate design of the nanoparticle array, the infrared SPR band can be made to be coincident with the SEIRA sensitive infrared bands of the PNBA. The trends in the infrared SPR peak frequencies and band shapes were consistent with predictions from electrodynamic theory. The SEIRA responses per unit area of deposited metal obtained with the PPA-type films were at best comparable to results obtained with disordered silver and gold films deposited on the same substrate materials by thermal evaporation (i.e., in the absence of any NSL masking spheres). The results of this study are most consistent with theories and models that attribute SEIRA to the dielectric constant and optical extinction spectrum of the metal film.

Index Headings: **Infrared spectroscopy; Surface-enhanced infrared absorption; Plasmon; SEIRA.**

INTRODUCTION

The intensification of infrared-active vibrational modes of molecules in close proximity to nanometer-thick metal films, commonly known as surface-enhanced infrared absorption (SEIRA), is receiving increased attention from both a phenomenological and practical viewpoint. Since the reporting of the first vestiges of SEIRA by Hartstein et al.[1] in 1980, numerous groups have attempted to interrogate the mechanistic aspects of SEIRA,[2–8] to employ it in analysis/characterization studies,[9–12] and to exploit it as a sensing tool.[13,14] Osawa et al.[2] and Johnson and Aroca[3] investigated electromagnetic models based on effective medium theories to (1) explain the coupling of surface plasmons intrinsic to the metal films with vibrational modes of molecules adsorbed on the films and (2) determine the expected enhancement factors. Their treatments took into consideration the size and shape of the metal islands that persist in most SEIRA-active metal films. Roseler and Korte,[4] on the other hand, interrogated nanometer-thick metal films by an ellipsometric method and showed that, for purposes of phenomenological treatment, the intrinsic optical properties of the films (refractive index and absorptivity) could be reproduced by assuming the films behave like isotropic layers of uniform thickness.

Merklin and Griffiths[5,6] reported results giving evidence that (1) the surface roughness/inhomogeneities found in typical vapor-deposited metal island films compromise the idealized selection rules postulated by Osawa et al.,[2] and (2) chemical effects (e.g., chemical attachment of the analyte molecule to the metal film) influence peak positions and relative intensities of SEIRA bands. Badilescu et al.[7] deduced from their measurements that infrared absorption enhancement is highly dependent on the molecular structure of the adsorbed molecules and is significantly greater for vibrations of polar groups having large dipole moment gradients. The optimum thickness for a SEIRA-active metal film shows some variability from study to study, but is consistently in the 4 to 10 nm range.[1–8] In a conceptually interesting study with mechanistic implications, Al-Rawashdeh and Foss[9] incorporated gold nanorods in polyethylene films and obtained a SEIRA-active embodiment with a discrete plasmon resonance absorption maximum in the near-infrared region.

The purpose of the investigation reported in this paper is to examine the SEIRA response of metal island films with architectures engineered to produce a discrete plasmon in the mid-infrared and to compare that response with the SEIRA activity exhibited by metal films having no discrete plasmon. The prior work of Van Duyne et al.[15,16] has shown that it is possible to create metal island arrays with controllable plasmon resonances having peak frequencies ranging from the visible spectral region to values well into the near IR. The methodology for doing this is based on the nanosphere lithography technique used by Hulteen and Van Duyne[17] to produce periodic particle arrays (PPAs) for surface-enhanced Raman spectroscopy (SERS) at excitation wavelengths between 400 and 900 nm.[16] The results reported herein extend this capability to the mid-IR region and have allowed us to compare detection sensitivities of SEIRA-optimized, vapor-deposited metal island films[14] with metal island arrays having peaked surface plasmon resonances that overlap the spectral frequencies of typical analyte molecules, such as *para*-nitrobenzoic acid.

EXPERIMENTAL

The disordered silver metal island films were deposited on silicon and germanium internal reflection elements

Received 21 August 1999; accepted 7 October 1999.
* Authors to whom correspondence should be sent.

0003-7028/00/5403-0371$2.00/0

(IREs) and on thin mica sheets by using a Denton (Model DV-515) thermal evaporator. The IRE dimensions were 25 mm × 5 mm × 2 mm, and in each case the metal films were applied to one of the 25 mm × 5 mm surfaces. The background pressure in the evaporator during deposition was always less than 10^{-5} torr. Nanogram quantities of the analyte molecule were applied to the surfaces of the IREs and the mica sheets by micro-syringe deposition of dilute solutions of the analyte in methylethyl ketone. Infrared spectra were recorded with a Bio-Rad FTS 185 Fourier transform infrared spectrometer. The IREs were positioned in the spectrometer by using a 4× attenuated total reflection (ATR) beam condenser (Harrick Scientific Corp.) configured to produce six reflections at each IRE surface. Each recorded spectrum consisted of 100 scans taken at 4 cm^{-1} resolution. Other details about the specific methodologies used in our laboratory to vapor deposit the metal island films, apply the analyte molecular layers, and record the infrared spectra are reported elsewhere.[14]

Periodic particle array films were fabricated by nanosphere lithography. The details of this method have been previously described.[17] The metal film type that will hereafter be referred to as the "base case" PPA film was prepared by drop-coating a suspension of 2540 ± 60 nm-diameter polystyrene nanospheres onto an IRE or thin mica substrate and allowing the nanospheres to self-assemble into a hexagonally close-packed monolayer. The samples were then mounted in the chamber of a Consolidated Vacuum Corporation vapor deposition system. With the use of the monolayer of nanospheres as a deposition mask, 50 nm of silver was deposited at normal incidence onto the samples at a rate of 0.2 nm/s. Film thickness and rate of deposition were measured with a Leybold Inficon quartz crystal microbalance deposition monitor (Model XTM/2). The chamber pressure during deposition was approximately 10^{-7} torr. Following the silver deposition, the nanosphere mask was removed by sonication in methylene chloride, leaving behind a hexagonal array of uniformly sized silver particles with triangular cross-sectional shapes.

Two variations on the base case PPA fabrication method were employed to increase the total substrate area covered with metal particles and to distort the array architecture: (1) angle-tuning and (2) multi-deposition. Angle-tuned PPA films were fabricated via three sequential depositions of Ag at varying angles of incidence onto a single nanosphere mask. First, 10 nm of Ag was deposited at normal (0°) incidence onto a substrate coated with 2540 nm-diameter polystyrene nanospheres. Then the angle of incidence was changed to +25° and a second 10 nm of Ag was deposited. Lastly, the angle of incidence was adjusted to −25°, and a third 10 nm Ag deposition was made. After these three depositions, the polystyrene nanosphere mask was removed.

Multi-deposition PPA films were made by performing three sequential depositions of Ag at a normal angle of incidence, each time with the use of a nanosphere mask with a different diameter. As a first step, 10 nm of Ag was deposited at normal incidence onto a substrate with a 2540 nm-diameter nanosphere mask. Then the nanospheres were removed and an aliquot of a suspension of 400 ± 7 nm-diameter polystyrene nanospheres was drop-coated onto the same substrate. The smaller nanospheres self-assembled within the template of the existing PPA and served as a mask for a second deposition of 10 nm of Ag. Once again, the nanosphere mask was removed and a suspension of 266 ± 8 nm-diameter nanospheres was drop-coated onto the substrate. After a third deposition of 10 nm of Ag, the nanosphere mask was removed.

Additional PPA films made with 2700 nm polystyrene nanospheres and 65 nm-thick silver deposits were applied to several Si and Ge IREs and to a Si wafer to investigate the effect of the metal island array parameters and infrared measurement method on plasmon frequency and SEIRA response. In one case, the silver deposit was made at a sufficiently steep angle (45°) relative to the substrate surface to prevent silver from passing the mask (i.e., no array was created). This was done to test the consequences to the SEIRA measurements of having a few large silver island deposits in places on the surface of the substrate where there were holes in the nanosphere mask due to incomplete packing of the polystyrene spheres. Such a test was considered necessary because several of these types of large globular deposits were seen on the surfaces of all PPA-coated substrates.

Atomic force microscopy (AFM) images were obtained with the use of a Digital Instruments Nanoscope III microscope equipped with etched silicon nanoprobe tips obtained from Digital Instruments. The tips were conical in shape with a cone angle of 20° and an effective radius of curvature at the tip of 10 nm. Their spring constant was approximately 0.15 Nm^{-1}. The AFM images presented herein represent raw, unfiltered data collected in the constant force mode. The lateral dimensions of the

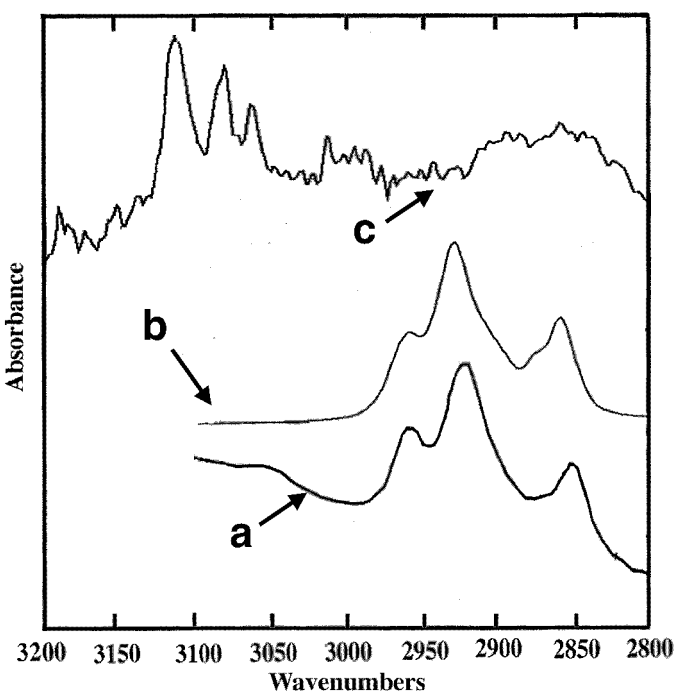

FIG. 1. (*a*) The ATR/SEIRA spectrum attributed to PNBA by Hartstein et al.;[1] (*b*) the ATR spectrum in the C–H stretching region of the type of vacuum pump oil employed in devices such as the Denton evaporator (obtained in our laboratory with the use of a germanium IRE); (*c*) the ATR spectrum in the C–H stretching region of PNBA deposited on a germanium IRE.

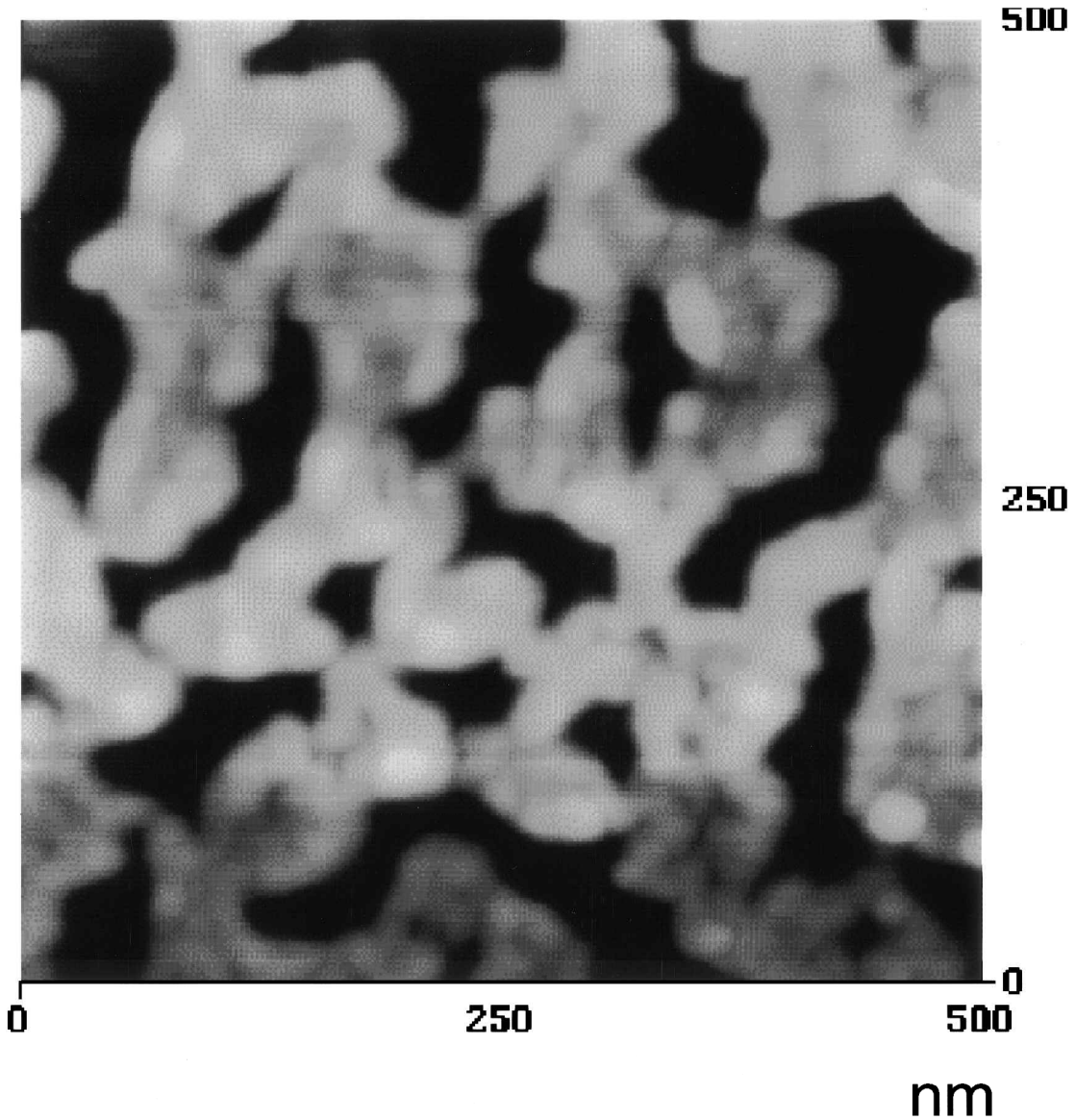

FIG. 2. AFM image of the type of disordered vapor-deposited metal island film (this one being silver on a germanium IRE) that gives optimum SEIRA activity as reported in Ref. 14.

particles were not corrected for any broadening caused by tip convolution.

The analyte molecule used in this study is *para*-nitrobenzoic acid (PNBA, Aldrich, reagent grade). PNBA has been widely used in studies of the SEIRA effect, most probably because it was the molecule of principal emphasis in the original paper by Hartstein et al.[1] In fact, some may not have recognized that the SEIRA spectrum of PNBA reported by Hartstein et al. appears to be that of a fully saturated hydrocarbon (possibly vacuum pump oil), not PNBA, as the group of infrared spectra in Fig. 1 tends to indicate.

RESULTS AND DISCUSSION

The disordered silver and gold metal island films, produced by thermal evaporation of the metal onto the surfaces of unmasked silicon, germanium, and mica substrates, had a globular, interconnected morphology typified by the AFM image in Fig. 2. Computer-assisted image analysis of the AFM height gray scale gave the metal film height (thickness) histogram shown in Fig. 3. This morphology on silicon and germanium IREs has produced SEIRA-induced detection sensitivity increases that exceed 500× for PNBA, based on prior work done in our laboratory.[14] Figure 4 presents a comparison of the SEIRA spectrum of PNBA on an optimized, vapor-deposited silver film supported on a germanium IRE and the normal ATR spectrum of a tenfold greater quantity of PNBA on a clean (metal film-free) germanium IRE. Spectra such as those in Fig. 4 allow the estimation of relative enhancements in the presence of and absence of a metal island film and are, therefore, independent of the number of ATR reflections, since all other measurement conditions are the same.

Figure 5 shows AFM images of the three different PPA film morphologies obtained with 2540 nm nanosphere masks (labeled ***a***, ***b***, and ***c***) on a mica substrate: ***a*** is the base case PPA, ***b*** is the angle-tuned PPA, and ***c*** is the

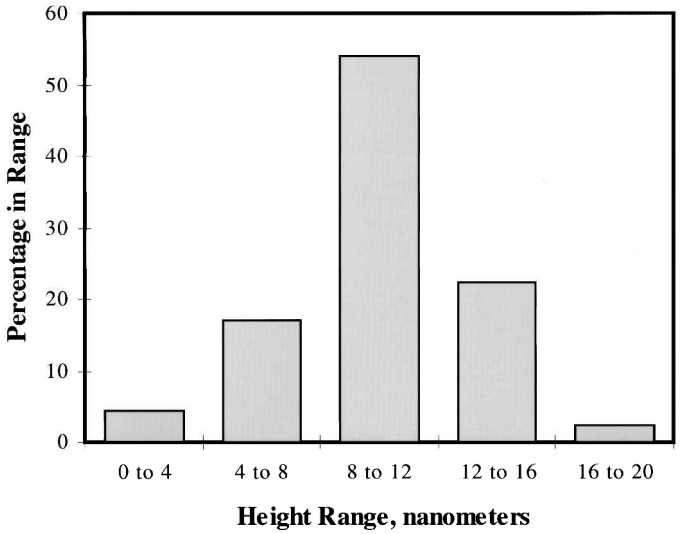

FIG. 3. Metal film thickness histogram obtained from the height gray scale for the AFM image shown in Fig. 2.

multi-deposition PPA, each produced by the respective method described in the Experimental section. The infrared absorbance spectra of each of the three PPA film architectures and a typical silver vapor-deposited metal island film were measured on germanium elements in

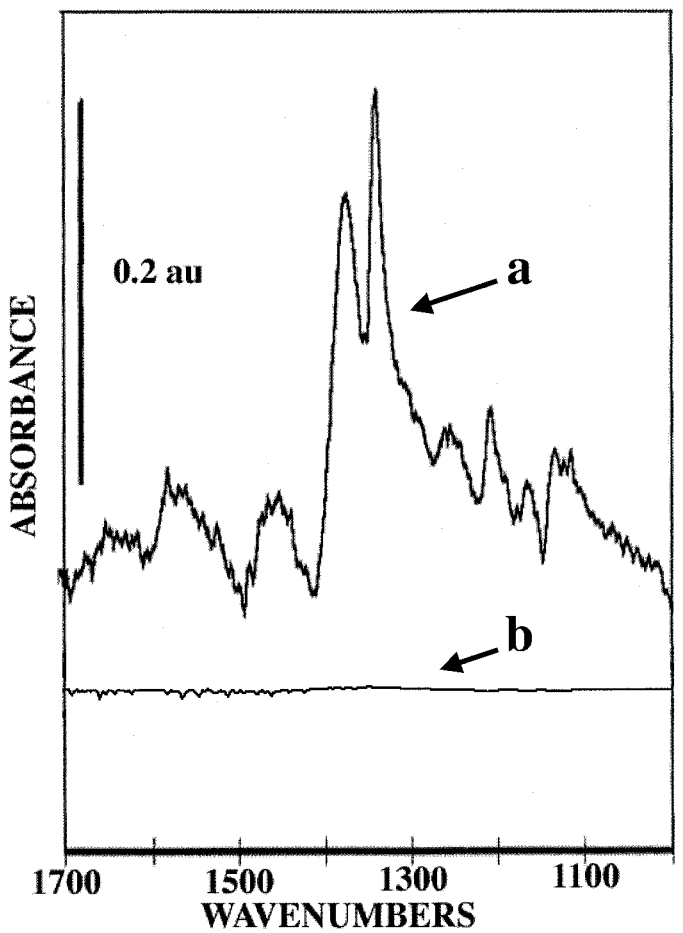

FIG. 4. (***a***) SEIRA spectrum of ~ 10 ng PNBA on a disordered vapor-deposited silver film supported on a clean germanium IRE. (***b***) Infrared spectrum of 100 ng of PNBA on a clean germanium IRE.

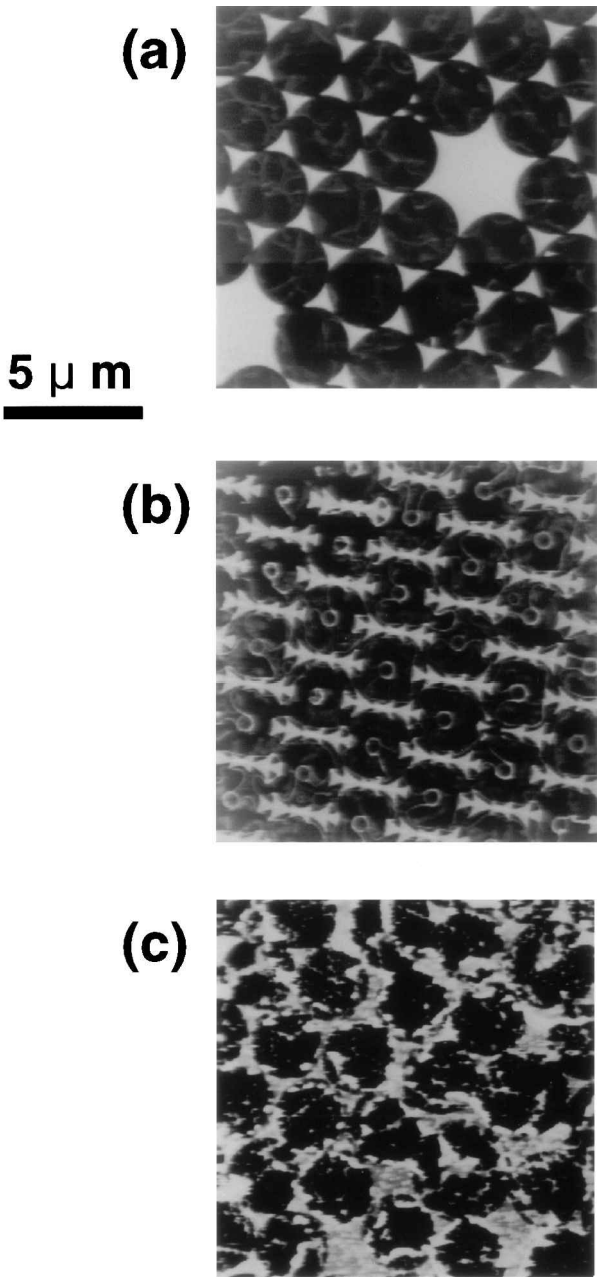

FIG. 5. AFM images (15 μm × 15 μm area) for (**a**) a base case PPA; (**b**) an angle-tuned PPA; (**c**) a multi-deposition PPA.

ATR mode. In addition, the absorbance spectrum of a base case PPA was measured on a silicon IRE and a thin mica substrate in order to probe the effect of the substrate. These results are displayed in Fig. 6, where we show in each case the difference spectrum obtained by subtracting the spectrum of the bare substrate from that of the metal-particle-array-coated substrate.

The spectrum of the base case PPA on a mica substrate in Fig. 6 was obtained in the transmission mode; all other spectra were obtained in the ATR mode. (The oscillatory pattern present in the transmission mode spectrum of the base case PPA on mica is due to interference of the infrared probe beam caused by the stratified layering of the mica substrate.) The peak frequency of the surface plasmon resonance for the base case PPA on the mica substrate is approximately 2932 cm^{-1}. This value is red-shift-

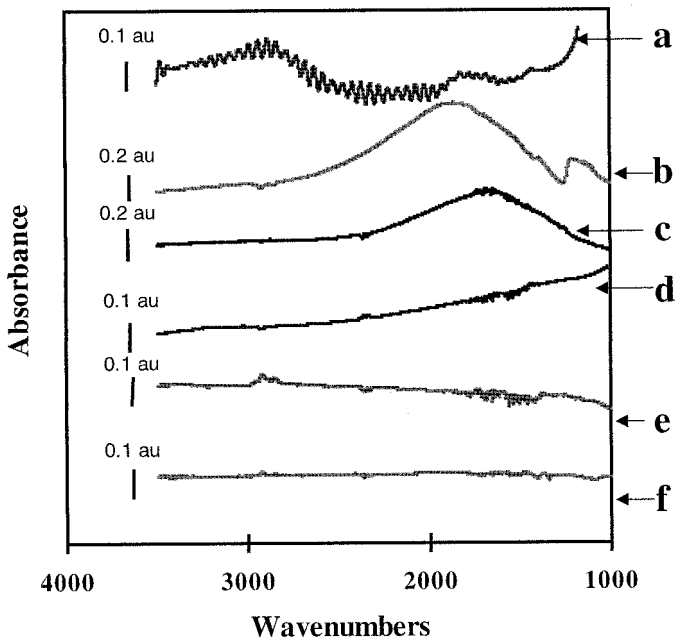

FIG. 6. Mid-IR absorption spectra of (***a***) a base case PPA on a mica substrate measured in transmission mode; (***b***) a base case PPA on a silicon IRE; (***c***) a base case PPA on a germanium IRE; (***d***) an angle-tuned PPA on a germanium IRE; (***e***) a multi-deposition PPA on a germanium IRE; (***f***) a vapor-deposited silver island film on a germanium IRE. Spectra ***b*** through ***f*** were measured in the ATR mode.

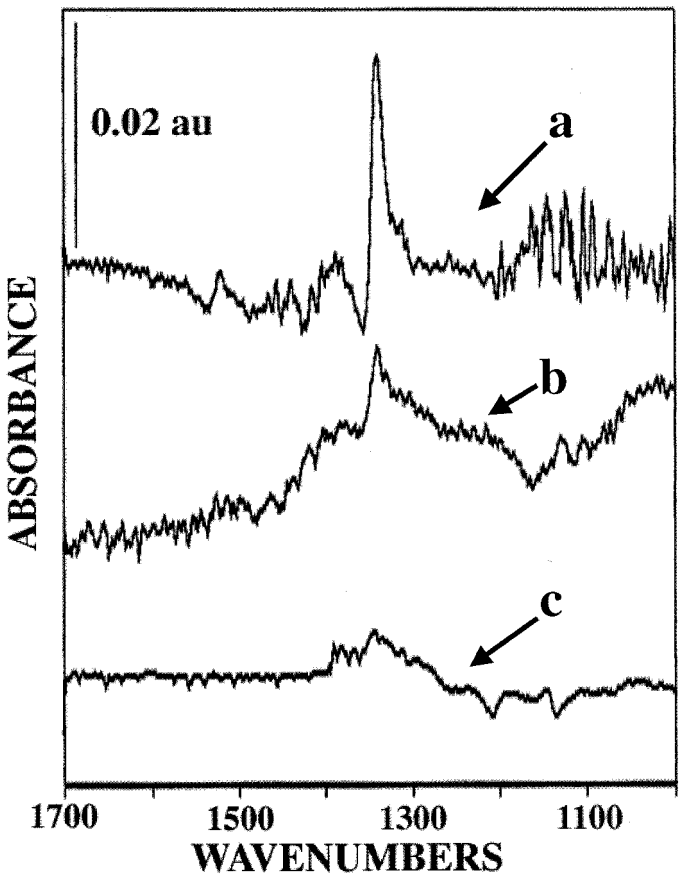

FIG. 7. SEIRA spectra of PNBA measured for base case PPA films on (***a***) a silicon IRE (~ 30 ng of PNBA applied) and (***b***) a germanium IRE (~ 10 ng of PNBA applied). (***c***) The infrared spectrum of ~ 100 ng PNBA on a clean germanium IRE.

ed for the base case PPA on the silicon IRE to 1870 cm^{-1}, and further red-shifted to 1655 cm^{-1} on the germanium IRE. The ATR spectrum of the angle-tuned PPA architecture on a germanium IRE appears to show a plasmon resonance that is even further red-shifted and considerably broadened. Since the particles in the angle-tuned PPA are closely coupled and more heterogeneous in size than in the base case PPA, this is a reasonable result. The multi-deposition PPA architecture and the typical vapor-deposited silver island film (both on germanium IREs) show no discrete plasmon resonance, as would be expected on the basis of the wide range of particle shapes and sizes present in the films.

SEIRA spectra of PNBA obtained for a base case PPA film on a silicon IRE and a germanium IRE are shown as curves ***a*** and ***b*** in Fig. 7, together with the spectrum of PNBA on a clean germanium IRE. The nitro group N–O symmetric stretch is the strongest peak visible in the two SEIRA spectra. We can make an approximate comparison of the relative SEIRA enhancement factor for the base case PPA film architecture to that of a typical vapor-deposited metal island film by taking account of the total substrate area covered by metal for each type of film and the SEIRA band intensity for a fixed amount of PNBA on one surface of our standard IRE. Optical microscope pictures and AFM images (e.g., Fig. 2) indicate that the metal surface coverage in a typical vapor-deposited metal island film on a germanium or silicon IRE surface is nominally around 70±10%. The SEIRA intensity of the nitro group N–O symmetric stretch band observed after application of a ~ 10 ng aliquot of PNBA to such a film on a 25 mm by 5 mm IRE surface is ~ 0.25 absorbance units.[14] This leads to a normalized SEIRA intensity of ~ 0.3 au per cm^2 of metal film for a 100% metal-covered IRE surface. The total substrate area covered by metal for a base case PPA film on a silicon or germanium IRE is about 2%, based on the known geometry, dimensions, and spacing of the particles and the observation from optical and AFM measurements that only about 20% of the IRE surface is actually embraced by the PPA array. (This partial coverage is a consequence of fixturing and masking requirements during PPA film deposition.) From this effective area estimation for a base case PPA and several sets of SEIRA measurements (like those in Fig. 7) on PPA-coated IREs, we deduce a normalized SEIRA intensity in the range 0.1 to 0.3 au per cm^2 of metal film for the N–O symmetric stretch after a 10 ng deposition of PNBA to an IRE surface coated with a base case PPA.

On the basis of the above estimation procedure, the SEIRA intensities on the PPA films appear to be comparable to those on the vapor-deposited metal island films, if we normalize each case to 100% metal coverage. In actual practice, the spacing between metal particles for each case is presumably essential to the SEIRA mechanism, and it is also quite likely that analyte molecules must be in contact with the metal particles to be SEIRA sensitized. Hence, while much can be learned about the mechanism of the SEIRA effect from the PPA studies, from a practical viewpoint the greater substrate surface coverage afforded by thermal evaporation onto unmasked substrates should make that method the more preferable

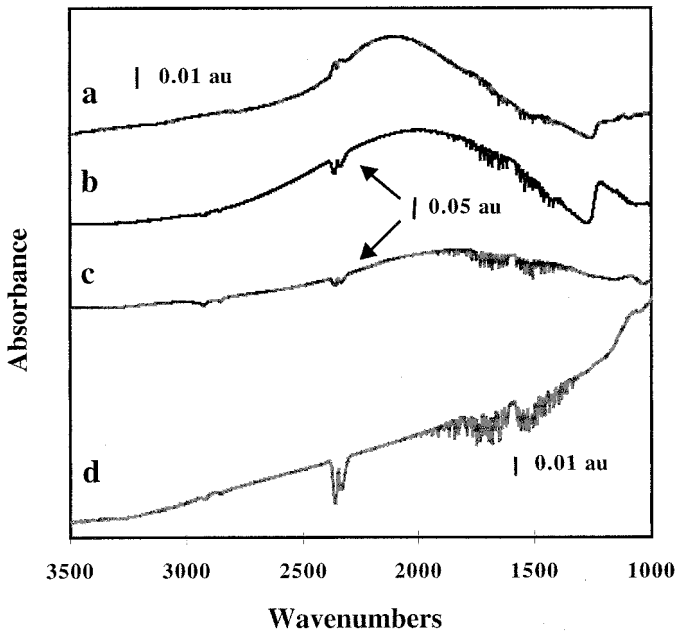

FIG. 8. Mid-IR absorption spectra of the 2700 nm-sphere-based PPA (with 65 nm thick Ag) on (***a***) a silicon wafer substrate (measured in transmission mode); (***b***) a silicon IRE (measured in the ATR mode); (***c***) a germanium IRE (measured in the ATR mode); (***d***) a germanium IRE on which the silver deposition angle was steep enough to prevent PPA formation (measured in the ATR mode).

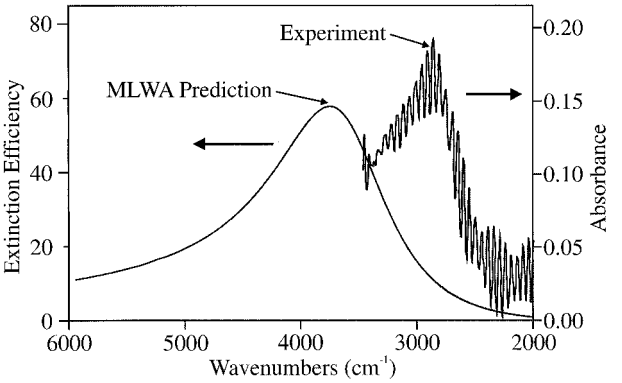

FIG. 9. Calculated extinction spectrum of a single oblate silver ellipsoid (major axis = 830 nm, minor axis = 50 nm) on a mica substrate (ordinate scale to the left) vs. the measured absorption spectrum of a base case silver PPA on mica (ordinate scale to the right).

one for practical applications of SEIRA (e.g., in chemical sensors).

The plasmon bands for the series of particle arrays made with 2700 nm nanospheres and a 65 nm silver deposit are shown in Fig. 8. The peak of the plasmon band for the PPAs on the Ge and Si IREs is shifted to slightly higher frequency compared to the base case PPAs on these same substrates. This observation can be rationalized by the electrodynamic theory[19] (and subsequent discussion herein), since the particles in the 2700 nm-based array have lower aspect ratios (897 nm: 65 nm = 13.8: 1) than those of the base case PPA (830 nm: 50 nm = 16.6:1). The plasmon peak obtained for the 2700 nm-based array by the ATR method (using the Si IRE) and by the transmission method (using the Si wafer) are essentially the same, showing that the frequency spectrum of a PPA plasmon band is not sensitive to infrared measurement technique. The steep angle-tuned sample that had no PPA (only scattered silver globules per optical microscope examination) had no plasmon, confirming that the peaked plasmons do indeed emanate from the particle arrays. Also, the SEIRA activities of the 2700 nm-based PPAs were roughly half those measured for the base case arrays on the same substrates, while the steep angle-tuned Ge IRE (the one with no particle array and no plasmon) showed no SEIRA activity.

Using electrodynamic theory we have modeled the surface plasmon resonance spectrum of a single particle on mica, germanium, and silicon substrates. The model employed is the modified long wavelength approximation (MLWA) developed by Zeman and Schatz and fully described elsewhere.[18,19] It is based on the electrostatic solution of Maxwell's equations, which is valid when the particle size is very small (<1%) compared to the wavelength of light. The electrostatic solution is corrected for electrodynamic effects through order $1/\lambda^3$, which extends the validity of the solution to particles that are up to 10% in size of the wavelength of light. These electrodynamic corrections can be described as radiative damping and dynamic depolarization. The effect of radiative damping is to increase the plasmon linewidth as particle size is increased, while dynamic depolarization will red-shift the position of the plasmon resonance as particle size is increased.

In order to apply the MLWA model to our system we approximate the shape of the particles in the PPA as oblate ellipsoids. We then input to the calculation the size of the ellipsoid and the dielectric constants of the metal of which the particle is composed. From AFM, the major axis of the particle (measured as the perpendicular bisector of the triangular base) is 830 nm, and the minor axis (measured as the height of the particle) is 50 nm. Wavelength-dependent bulk dielectric constants for silver from Palik[20] are used. The results of these MLWA calculations are presented as extinction efficiencies, which are the ratio of the calculated extinction cross sections to the cross-sectional area of a sphere whose volume is equal to that of the oblate ellipsoid.[16]

Figure 9 shows the calculated surface plasmon resonance spectrum of a single oblate ellipsoid on a mica substrate vs. the measured absorbance (or more accurately, extinction) of a base case PPA on mica. The linewidths of the calculated and measured peaks are similar, although the peak plasmon resonance frequencies differ by approximately 1000 cm^{-1}. This match is surprisingly good considering that the particle size is greater than 10% of the wavelength of the incident light. There are two factors in the experimental conditions that have not been addressed in the calculation. The first of these is that only a single particle has been used to model the optical response of the collection of particles comprising the PPA. We would expect some degree of particle–particle interaction that would red-shift the plasmon resonance relative to the plasmon resonance of a single particle. Secondly, we have made the approximation that the particles are oblate ellipsoids in shape, when in fact they are triangular in cross section.

The calculated effect of the underlying substrate is

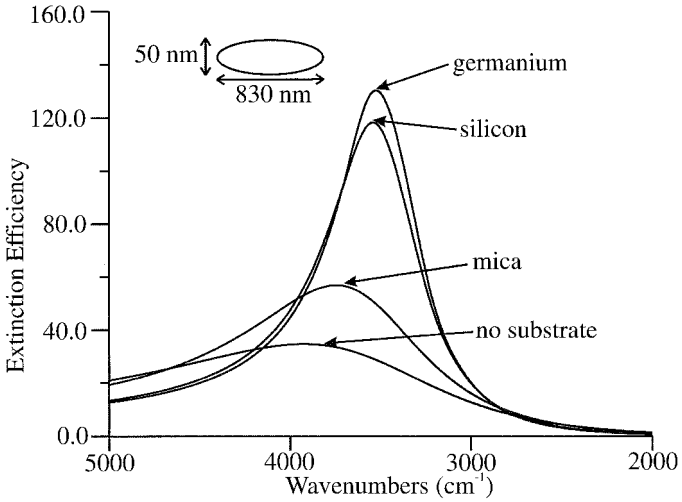

FIG. 10. Calculated extinction spectra of an oblate silver ellipsoid with no substrate (ϵ_{subst} = 1.0), a mica substrate (ϵ_{subst} = 2.5), a silicon substrate (ϵ_{subst} = 11.7), and a germanium substrate (ϵ_{subst} = 16.0).

shown in Fig. 10. The surface plasmon resonance of an oblate ellipsoid directly in contact with a substrate red-shifts and increases in magnitude as the dielectric constant of the substrate is increased. Experimentally, we observed red-shifting of the absorbance peak with increasing substrate dielectric constant as theory predicts. And in general, although the magnitude of the shift is much greater than that predicted by theory, the modeling results appear to be in reasonably good semiquantitative agreement with the observations.

CONCLUSION

We find from the work reported above that it is indeed possible to produce metal island films with discrete mid-IR plasmon resonances using the PPA technique. The trends in the peak frequencies and band shapes of these resonances for the silicon, germanium, and mica substrates are consistent with theoretical predictions. While the PPA-type metal island films do exhibit SEIRA activity, we have observed no exceptional advantages (i.e., in terms of significantly greater enhancements per unit area of metal) compared to disordered metal island films. In general, our results are most consistent with theories and models that attribute SEIRA to the dielectric constant and optical extinction coefficient of the metal film producing the effect. The importance of the band shape and frequency domain of plasmon resonance waves in determining the degree of SEIRA activity is not completely clear from our work, nor are the relative contributions of electromagnetic effects and molecular orientation effects. It is also abundantly clear from our collective experience with the SEIRA process that an exact method for determining the absolute magnitude of the infrared absorption enhancement associated with a metal-film-coated substrate relative to that of an uncoated substrate remains to be developed.

ACKNOWLEDGMENTS

G. W. Zajac (Amoco Corp.) performed some of the initial AFM measurements on vapor-deposited metal films, and A. K. Fischer (Argonne National Laboratory) contributed to the compilation and analysis of the AFM and infrared spectral data. The authors also wish to acknowledge helpful discussions with G. C. Schatz (Northwestern University) and to thank Bio-Rad Digilab Division for the loan of the FTS-185 FT-IR spectrometer used in this work. The research at Argonne National Laboratory was sponsored by the U.S. Department of Energy under Contract W-31-109-ENG-38 and at Northwestern University by grants from the ARO (Grant DAAG55-97-1-0133), the NSF (Grant CHE-940078), and the MRSEC Program of the NSF (Grant DMR-9632472).

1. A. Hartstein, J. R. Kirtly, and J. C. Tsang, Phys. Rev. Lett. **45,** 201 (1980).
2. M. Osawa, K. Ataka, K. Yoshii, and Y. Nishikawa, Appl. Spectrosc. **47,** 1497 (1993).
3. E. Johnson and R. Aroca, J. Phys. Chem. **99,** 9325 (1995).
4. A. Roseler and E.-H. Korte, Appl. Spectrosc. **51,** 902 (1997).
5. G. T. Merklin and P. R. Griffiths, J. Phys. Chem. **101,** 5810 (1997).
6. G. T. Merklin and P. R. Griffiths, Langmuir **13,** 6159 (1997).
7. S. Badilescu, P. V. Ashrit, V. Truong, and I. I. Badilescu, Appl. Spectrosc. **43,** 549 (1989).
8. H. D. Wanzenbock, B. Mizaikoff, G. Friedbacher, M. Grasserbauer, R. Kellner, M. Arntzen, T. Luyven, W. Theiss, and P. Grosse, Mikrochim. Acta **14,** 665 (1997).
9. N. Al-Rawashdeh and C. A. Foss, Jr., Nanostruct. Mater. **9,** 383 (1997).
10. S. Sato and T. Suzuki, Appl. Spectrosc. **51,** 1170 (1997).
11. N. Makino, K. Mukai, and Y. Kataoka, Appl. Spectrosc. **51,** 1460 (1997).
12. M. Osawa and K. Yoshii, Appl. Spectrosc. **51,** 512 (1997).
13. R. Kellner, B. Mizaikoff, M. Jakusch, H. D. Wanzenbock, and N. Weissenbacher, Appl. Spectrosc. **51,** 495 (1997).
14. S. A. Johnson, N.-H. Pham, V. J. Novick, and V. A. Maroni, Appl. Spectrosc. **51,** 1423 (1997).
15. J. C. Hulteen, D. A. Treichel, M. T. Smith, M. L. Duval, T. R. Jensen, and R. P. Van Duyne, J. Phys. Chem. B. **103,** 3854 (1999).
16. T. R. Jensen, G. C. Schatz, and R. P. Van Duyne, J. Phys. Chem. B. **103,** 2394 (1999).
17. J. C. Hulteen and R. P. Van Duyne, J. Vac. Sci. Technol., A **13,** 1553 (1995).
18. T. R. Jensen, L. Kelly, A. Lazarides, and G. C. Schatz, J. Cluster Sci. **10,** 295 (1999).
19. E. J. Zeman and G. C. Schatz, J. Phys. Chem. **91,** 634 (1987).
20. E. D. Palik, *Handbook of Optical Constants of Solids* (Academic Press, New York, 1985).